

Long-range surface polaritons in ultra-thin films of silicon

V. Giannini, Y. Zhang, M. Forcales and J. Gómez Rivas

FOM Institute for Atomic and Molecular Physics AMOLF, c/o Philips Research Laboratories,
High Tech Campus 4, 5656 AE, Eindhoven, The Netherlands.

giannini@amolf.nl

www.nanowirephotonics.com

Abstract: We present an experimental and theoretical study of the optical excitation of long-range surface polaritons supported by thin layers of amorphous silicon (a-Si). The large imaginary part of the dielectric constant of a-Si at visible and ultraviolet (UV) frequencies allows the excitation of surface polariton modes similar to long-range surface plasmon polaritons on metals. Propagation of these modes along considerable distances is possible because the electric field is largely excluded from the absorbing thin film. We show that by decreasing the thickness of the Si layer these excitations can be extended up to UV frequencies, opening the possibility to surface polariton UV optics compatible with standard Si technology.

© 2008 Optical Society of America

OCIS codes: (240.0240) Optics at surfaces; (240.0310) Thin films; (240.5420) Polaritons.

References and links

1. R. Ruppin and R. Englman, "Optical phonons of small crystals," *Rep. Prog. Phys.* **33**, 149–196 (1970).
2. D. L. Mills and E. Burstein, "Polaritons: the electromagnetic modes of media," *Rep. Prog. Phys.* **37**, 817–926 (1973).
3. A. V. Zayats, I. I. Smolyaninov, and A. A. Maradudin, "Nano-optics of surface plasmon polaritons," *Phys. Rep.* **408**, 131–314 (2005).
4. W.L. Barnes, A. Dereax, and T. W. Ebbesen, "Surface plasmon subwavelength optics," *Nature* **424**, 824–830 (2003).
5. J.-C. Weeber, J.R. Krenn, A. Dereux, B. Lamprecht, Y. Lacroute, and J.P. Goudomet, "Near-field observation of surface plasmon polariton propagation on thin metal film stripes," *Phys. Rev. B* **64**, 045411 (2001).
6. S. I. Bozhevolnyi, J. Erland, K. Leosson, P. M. W. Skovgaard, and J.M. Hvam, "Waveguiding in surface plasmon polariton band gap structures," *Phys. Rev. Lett.* **86**, 3008–3011 (2001).
7. S. I. Bozhevolnyi, V. S. Volkov, E. Devaux, and T. W. Ebbesen, "Channel plasmon-polariton guiding by sub-wavelength metal grooves," *Phys. Rev. Lett.* **95**, 046802 (2005).
8. B. Steinberger, A. Hohenau, H. Ditlabacher, A. L. Stepanov, A. Drezet, F. R. Aussenegg, A. Leitner, and J. R. Krenn, "Dielectric stripes on gold as surface plasmon waveguides," *App. Phys. Lett.* **88**, 094104 (2006).
9. A. V. Krasavin and A. V. Zayats, "Passive photonic elements based on dielectric-loaded surface plasmon polariton waveguides," *App. Phys. Lett.* **90**, 211101 (2007).
10. R. F. Oulton, V. J. Sorger, D. A. Genov, D. F. P. Pile and X. Zhang, "A hybrid plasmonic waveguide for subwavelength confinement and long-range propagation," *Nature Photonics* **2**, 496–500 (2008).
11. E. N. Economou, "Surface plasmons in thin films," *Phys. Rev.* **182**, 539–554 (1969).
12. D. Sarid, "Long-range surface-plasma waves on very thin metal films," *Phys. Rev. Lett.* **47**, 1927–1930 (1981).
13. J. C. Quail, J. G. Rako, and H. J. Simon, "Long-range surface-plasmon modes in silver and aluminum films," *Opt. Lett.* **8**, 377–379 (1983).
14. J. J. Burke, G. I. Stegeman, and T. Tamir, "Surface-polariton-like waves guided by thin, lossy metal films," *Phys. Rev. B* **33**, 5186–5201 (1986).
15. R. Charbonneau, P. Berini, E. Berolo, and E. Lisicka-Shrzek, "Experimental observation of plasmon-polariton waves supported by a thin metal film of finite width," *Opt. Lett.* **25**, 844–846 (2000).

16. T. Nikolajsen, K. Leosson, I. Salakhutdinov, and S. I. Bozhevolnyi, "Polymer-based surface-plasmon-polariton stripe waveguides at telecommunication wavelengths," *App. Phys. Lett.* **82**, 668–670 (2003).
17. F. Yang, J. R. Sambles, and G. W. Bradberry, "Long-Range Coupled Surface Exciton Polaritons," *Phys. Rev. Lett.* **64**, 559–562 (1990).
18. F. Yang, G. W. Bradberry, and J. R. Sambles, "Experimental observation of surface excitation-polaritons on vanadium using infrared radiation," *J. Mod. Phys.* **37**, 1545–1553 (1990).
19. F. Yang, J. R. Sambles, and G. W. Bradberry, "Long-Range surface modes supported by thin films," *Phys. Rev. B* **44**, 5855–5872 (1991).
20. E. L. Wood, J. R. Sambles, F. A. Pudonin, and V. Yakovlev, "Degenerate long range surface modes, supported on thin nickel films," *Opt. Commun.* **132**, 212–216 (1996).
21. M. Takabayashi, M. Haraguchi, and M. Fukui, "Propagation length of guided waves in lossy Si film sandwiched by identical dielectrics," *J. Opt. Soc. Am. B* **12**, 2406–2411 (1995).
22. T. W. Ebbesen, H. J. Lezec, H. F. Ghaemi, T. Thio, and P. A. Wolff, "Extraordinary Optical Transmission through Sub-Wavelength Hole Arrays," *Nature* **391**, 667–669 (1998).
23. H. J. Lezec and T. Thio, "Diffracted evanescent wave model for enhanced and suppressed optical transmission through subwavelength hole arrays," *Opt. Express* **12**, 3629–3651 (2004).
24. M. Sarrazin and J.-P. Vigneron, "Optical properties of tungsten thin films perforated with a bidimensional array of subwavelength holes," *Phys. Rev. E* **68**, 016603 (2003).
25. F. Miyamaru, M. Tanaka, and M. Hangyo, "Resonant electromagnetic wave transmission through strontium titanate hole arrays with complex surface waves," *Phys. Rev. B* **74**, 115117 (2006).
26. E. Popov, S. Enoch, and M. Neviere, "Plasmon surface waves and complex-type surface waves: comparative analysis of single interfaces, lamellar gratings, and two-dimensional hole arrays," *Appl. Opt.* **46**, 154–160 (2005).
27. M.-W. Chu, C.-H. Chen, F. J. García de Abajo, J.-P. Deng, and C.-Y. Mou, "Surface exciton polaritons in individual Au nanoparticles in the far-ultraviolet spectral regime," *Phys. Rev. B* **77**, 245402 (2008).
28. E. Ozbay, "Plasmonics: merging photonics and electronics at nanoscale dimensions," *Science* **311**, 189–193 (2006).
29. J. D. Jackson, *Classical Electrodynamics* (Wiley, New York, 1975).
30. D. W. Lynch and W. R. Hunter, *Handbook of optical constants of solids*, Edited by E. D. Palik (Academic Press, New York, 1985).
31. P. Berini, "Figures of merit for surface plasmon waveguides," *Opt. Express* **14**, 13030–13042 (2006).
32. R. Buckley and P. Berini, "Figures of merit for 2D surface plasmon waveguides and application to metal stripes," *Opt. Express* **15**, 12174–12182 (2007).
33. J. Dostalek, A. Kasry, and W. Knoll, "Long range surface plasmons for observation of biomolecular binding events at metallic surfaces," *Plasmonics* **2**, 97–106 (2007).

1. Introduction

A polariton is an electromagnetic wave coupled to a polarization excitation in matter [1, 2]. When this coupled excitation is bound to the interface between two media it is called a surface polariton [3]. A surface polariton is an evanescent electromagnetic wave that propagates along the interface and with an amplitude decaying exponentially into the two media. Surface polaritons are named surface plasmon polaritons (SPPs) when one of the media is a metal and the other a dielectric. The continued scaling down of integrated circuits has led to an increasing interest in surface plasmon optics or plasmonics as a mean to guide electromagnetic waves confined into sub-wavelength distances to surfaces [4] - [10]. A limitation of plasmonic circuits is the relatively large damping of SPPs on metals at optical and UV frequencies, which leads to a short propagation length [4]. A way to overcome this limitation and to increase the propagation length is to couple surface polaritons on opposite sides of thin films [11, 12]. These coupled modes, named long-range surface plasmon polaritons in the case of metallic films, have a reduced damping due to the exclusion of the electric field from the absorbing layer and the larger penetration of this field into the surrounding non-absorbing dielectric.

Long-range surface polaritons (LRSPs) have been thoroughly investigated in thin metallic films [11] - [16]. There is, however, little work on surface polaritons supported by thin films of absorbing dielectrics. In the pioneering work of Yang *et al.* [17], it was demonstrated the excitation of LRSPs in thin films of vanadium at infrared wavelengths at which this material behaves as a strongly absorbing dielectric. In subsequent works, the same group demonstrated the exci-

tation of these modes in other materials such as palladium, organic films and islandised metallic films [18] - [20]. Takabayashi *et al.* measured the propagation of guided modes in thin slabs of Si at 633 nm [21]. However, at this wavelength the absorption of Si is weak and the modes investigated by Takabayashi and co-workers were more likely TM_0 modes rather than LRSPs. The phenomenon of enhanced optical transmission through arrays of subwavelength holes in thin metallic films [22], which is interpreted in terms of the excitation of surface modes, has triggered several studies on similar arrays structured in thin absorbing layers [23] - [26]. Very recently, the excitation of surface polaritons in Au nanoparticles has been also demonstrated in the extreme UV by means of electron energy-loss spectroscopy [27]. At these frequencies Au behaves as a strongly absorbing dielectric.

Here, we demonstrate that it is possible to excite long-range surface polaritons (LRSPs) in ultra-thin layers of amorphous Si (a-Si) at frequencies at which a-Si is a strongly absorbing dielectric, i.e., frequencies at which Si has a positive real component of the permittivity and a large imaginary component. These modes on films of a-Si have similar or even superior characteristics to those on gold films, with longer propagation lengths and similar confinement to the thin film. These important characteristics of LRSPs in Si layers will allow the scaling down of surface polariton circuits using well-known standard Si manufacturing processes. Moreover, Si is the most thoroughly investigated semiconductor and the ability to deposit with high precision atomically flat layers of this semiconductor, combined with the possibility of exciting surface modes on ultra-thin layers, could have important implications in several fields, including photovoltaics, near-field microscopy, optical data storage, optical lithography and sensing [28].

The manuscript is organized as follows. In section 2 we review theoretically the excitation of surface polaritons in thin films and compare the propagation length and the mode confinement in gold and a-Si. In section 3 we demonstrate experimentally with attenuated total reflection measurements the excitation of LRSPs in thin films of a-Si deposited on SiO_2 substrates. These measurements are compared to calculations using Fresnel theory. The conclusions are presented in section 4 .

2. Surface modes in thin films

The system that we are going to study is a thin film parallel to the x-y plane with thickness d and extending from $0 < z < d$. The film is made of a material with a complex permittivity $\epsilon = \epsilon_r + i\epsilon_i$ and it is surrounded by a non-absorbing and homogeneous medium with permittivity ϵ_d (see Fig. 1). Surface polaritons at the two interfaces of the thin film can couple when its thickness is smaller than the penetration length of the field. This coupling hybridizes the two surface polariton modes into two new modes called long-range surface polaritons (LRSPs) and short-range surface polaritons (SRSPs), respectively. LRSPs have a tangential component of the electric field to the film (E_x component in the system of coordinates defined in Fig. 1), which is asymmetric with respect to the middle plane of the film, i.e., the $z = d/2$ plane in Fig. 1. This field component vanishes inside the thin film and LRSPs have longer propagation lengths than that of surface polaritons on single interfaces due to their weaker interaction with the absorbing material. On the other hand, SRSPs have a tangential electric field component symmetric to the plane $z = d/2$ and a maximum field amplitude in the absorbing film, which leads to a shorter propagation length.

The general solution for the H_y magnetic field component of a TM polarized electromagnetic mode bounded at the interfaces, i.e., exponentially decaying into the dielectric, and propagating in the x direction, is given by [3]

$$H_y(x, y, z) = A_1 e^{-\alpha_d z} e^{i(kx - \omega t)} \quad \text{for} \quad z > d, \quad (1)$$

$$H_y(x, y, z) = [A_2 e^{-\alpha z} + A_3 e^{\alpha z}] e^{i(kx - \omega t)} \quad \text{for} \quad 0 \leq z \leq d, \quad (2)$$

$$H_y(x, y, z) = A_4 e^{\alpha_d z} e^{i(kx - \omega t)} \text{ for } z < 0, \quad (3)$$

where A_i ($i = 1 \dots 4$) are the field amplitudes, which are determined by the electromagnetic boundary conditions, and α_d and α are given by

$$\alpha_d^2 = k^2 - k_0^2 \epsilon_d, \quad (4)$$

$$\alpha^2 = k^2 - k_0^2 \epsilon, \quad (5)$$

where k_0 is the wave vector in vacuum and $k = k_r + ik_i$ is the complex propagation constant of the mode in the x direction. According to Eqs.(1)-(3), for modes bounded to the thin film is required that $Re(\alpha_d) > 0$. This condition is only fulfilled for non-absorbing films ($\epsilon = \epsilon_r$), when $k > k_0 \epsilon_d^{1/2}$ (see Eq.(4)). If the thin film is absorbing, $Re(\alpha_d)$ is positive when $Im(k) > 0$ [17, 18].

The confinement of the electromagnetic field to the surface of the film is defined by the intensity decay length into the surrounding dielectric

$$L_z = \frac{1}{2Re(\alpha_d)}. \quad (6)$$

The field intensity decays in the x -direction with a characteristic propagation length L_x given by

$$L_x = \frac{1}{2k_i}. \quad (7)$$

Imposing the electromagnetic boundary condition to Eqs.(1)-(3) we find the dispersion relations for LRSPs

$$\tanh\left[\frac{\alpha d}{2}\right] = -\frac{\epsilon \alpha_d}{\epsilon_d \alpha}. \quad (8)$$

Similarly to LRSPs, the dispersion relation of SRSP modes is given by

$$\tanh\left[\frac{\alpha d}{2}\right] = -\frac{\epsilon_d \alpha}{\epsilon \alpha_d}. \quad (9)$$

The real (k_r) and imaginary (k_i) components of the complex propagation constant of LRSP and SRSP modes are displayed in Figs. 2(a) and 2(b) as a function of the thickness of the layer with blue solid (LRSPs) and red dashed (SRSPs) curves. The values of k_r and k_i in these figures are normalized by the wave number in the surrounding dielectric $k_0 n_d$, where we have assumed

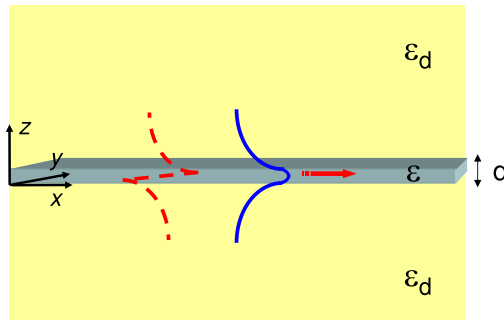


Fig. 1. Schematic representation of the electric field component along the x -direction of a long-range (red dashed curve) and of a short-range (blue solid curve) surface polariton in a thin layer of a material of permittivity ϵ surrounded by a dielectric of permittivity ϵ_d .

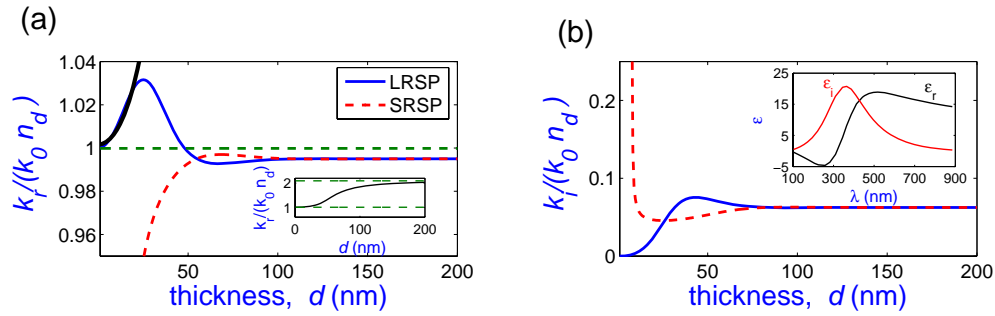


Fig. 2. (a) real k_r and (b) complex k_i components of the wave number of long-range surface polaritons (blue solid curves) and short-range surface polaritons (red dashed curves) in a-Si films at $\lambda_0 = 318$ nm as a function of the thickness of the film. The film is surrounded by a dielectric with a refractive index $n_d = \sqrt{\epsilon_d} = 1.45$. k_r and k_i are normalized to the wave number in the surrounding dielectric. The black curve and the inset in (a) represent the normalized wave number of the TM_0 mode in a non-absorbing thin film surrounded by a medium with $n_d = 1.45$. Inset of (b): wavelength dependence of the real (black curve) and imaginary (red curve) components of the permittivity of a-Si.

$n_d = \sqrt{\epsilon_d} = 1.45$. For the calculations of Figs. 2(a) and 2(b) we have considered the permittivity of the thin layer to be purely imaginary with a value of $\epsilon = 18.5i$, which corresponds to the permittivity of a-Si at $\lambda_0 = 318$ nm. The values of the permittivity of a-Si in the UV, visible and near-infrared are displayed in the inset of 2(b) [30].

For LRSPs and small values of film thickness, k_r is greater than $k_0 n_d$, i.e., $k_r/(k_0 n_d) > 1$ in Fig. 2(a), in contrast to the smaller values of k_r of SRSPs. In this situation it is necessary to enhance the momentum of incident light to couple to this long-range guided mode. Another important difference between LRSP and SRSP modes is the dependence of k_i for small values of d (Fig. 2(b)). For LRSPs k_i tends to zero as d vanishes, in contrast to the divergence of k_i of SRSPs for small d .

At this point it is useful to review the different types of long-range guided modes supported by thin films symmetrically surrounded by a non-absorbing dielectric. These modes can be classified according to the values of the complex permittivity of the thin layer. Long-range surface plasmon polaritons exist when the permittivity has a negative real value and a small imaginary value ($|\epsilon_r| \gg \epsilon_i \approx 0$) and $|\epsilon_r| > \epsilon_d$ [3]. TM_0 modes are supported by films of positive permittivity in which $\epsilon_r \gg \epsilon_i \approx 0$ and $\epsilon_r > \epsilon_d$ [29]. As mentioned above, for strongly absorbing thin films in which $|\epsilon_r| \lesssim \epsilon_i$ (independent of the sign of ϵ_r) and $\epsilon_i \gg 1$, there are also guided modes that can propagate many wavelengths [19]. These modes arise from the coupling of surface polaritons at the opposite sides of the absorbing layer. Note that there is an important difference between a generic TM_0 guided mode and LRSPs. A TM_0 mode is a bulk mode resulting from the interaction of the fields at the two surfaces of the thin film by means of total internal reflection; it is not a mode due to the coupling between two surface modes at opposite interfaces. In fact, for the permittivity range in which TM_0 modes exist, i.e., $\epsilon_i \approx 0$, there are no surface modes at the interface between two semi-infinite media [19]. To illustrate further the similitude and difference of TM_0 modes in non-absorbing layers and LRSPs in thin absorbing films, we have plotted in Fig. 2(a) with a black solid curve and in the inset of Fig. 2(a) the normalized wave number of the TM_0 mode in a layer of medium with $n = 3.0$, i.e., with a refractive index equal to the real value of the refractive index of a-Si at $\lambda_0 = 318$ nm, surrounded by a dielectric with $n_d = \sqrt{\epsilon_d} = 1.45$. The wave numbers of the TM_0 and the LRSP modes are similar for values of the film thickness smaller than 25 nm, indicating also

the similar characteristics of these two modes for these thickness. However, the wave numbers differ significantly for larger values of d . For $d \rightarrow \infty$ the wave number of the LRSP converges to that of a surface polariton on a single interface, while the wave number of the TM_0 mode converges to $k_0 n$.

The propagation length L_x at $\lambda_0 = 318$ nm of LRSPs calculated for a-Si films surrounded by a dielectric with $n_d = 1.45$ is displayed in Fig. 3(a)(blue solid curve) as a function of the thickness of the film. For comparison we have also plotted in Fig. 3(a) the propagation length of LRSPs in similar thin films of gold (red solid curve) at $\lambda_0 = 318$ nm, and for a-Si and gold at $\lambda_0 = 650$ nm (blue and red dashed curves respectively). In general L_x decreases as the thickness of the film increases, approaching the values of surface polaritons at single interfaces. A remarkable behavior is found by comparing the propagation lengths in these two media (see also inset of Fig. 3(a)): L_x in the case of a-Si films is close to or in general longer than the propagation length in Au in spite to be commonly accepted that metals are superior for the propagation of long-range polaritons. The values of the permittivity of Au and a-Si are displayed in table 1 for $\lambda_0 = 318, 450$ and 650 nm, together with the values of L_x for a film of thickness $d = 5$ nm. It should be pointed out that the guided mode in a-Si at $\lambda_0 = 650$ nm, with a remarkable long propagation length, corresponds to the TM_0 mode in the weakly absorbing layer at this wavelength.

The decay lengths of these modes in the surrounding dielectric L_z are displayed in Fig. 3(b) as a function of the thickness of the thin layer and in table 1 for $d = 5$ nm. These decay lengths illustrate the mode confinement to the film. Again, very similar values of L_z are found for Au and a-Si in the UV and in the visible. As the thickness of the thin layer is reduced, the mode is excluded from this layer decaying a longer distance into the dielectric.

The figure of merit (FOM) describing the quality of waveguiding structures can be defined as the ratio between the propagation length and the decay length into the surrounding dielectric L_x/L_z [31, 32]. Large values of this FOM indicate the preferable situation of a long propagation length and strong field confinement. The FOM is displayed in Fig. 3(c) for silicon (thin blue curves) and gold (thick red curves) at $\lambda_0 = 318$ nm (full curves) and at $\lambda_0 = 650$ nm (dashed curves). In general, due to the strong increase of L_x for small values of d , the FOM increases in spite of the also larger values of L_z . At $\lambda_0 = 318$ nm the performance of a-Si thin films is better than that of gold. At $\lambda_0 = 650$ nm similar FOMs are obtained only for the thinnest layers. The FOM represented in Fig. 3(c) correspond to calculations considering thin films without roughness. Surface roughness, inherent to real systems, will reduce L_x . However, as we will see later, it is possible to sputter very thin layers of a-Si (~ 10 nm) with high precision and with a roughness in the sub-nanometer range.

In order to illustrate further the reason why long propagation lengths are possible for LRSPs modes on thin films of strongly absorbing media, we have calculated the Poynting vector of the

Table 1. Characteristic lengths of long-range guided modes in a film with a thickness of 5 nm of amorphous Si and gold surrounded by a dielectric with refractive index $n_d = \sqrt{\epsilon_d} = 1.45$. Calculated values of propagation length L_x and decay length L_z into the dielectric at three different wavelengths $\lambda_0 = 318, 450$ and 650 nm. The permittivities of the materials at these wavelengths are also listed.

λ_0 (nm)	a-Si			Au		
	ϵ	L_x (μm)	L_z (nm)	ϵ	L_x (μm)	L_z (nm)
318	$0 + 18.5i$	26	216	$-0.2 + 7.0i$	10	194
450	$17.6 + 13.5i$	157	485	$-1.26 + 5.7i$	24	356
650	$17.3 + 3.0i$	1323	1112	$-9.7 + 1.0i$	1045	825

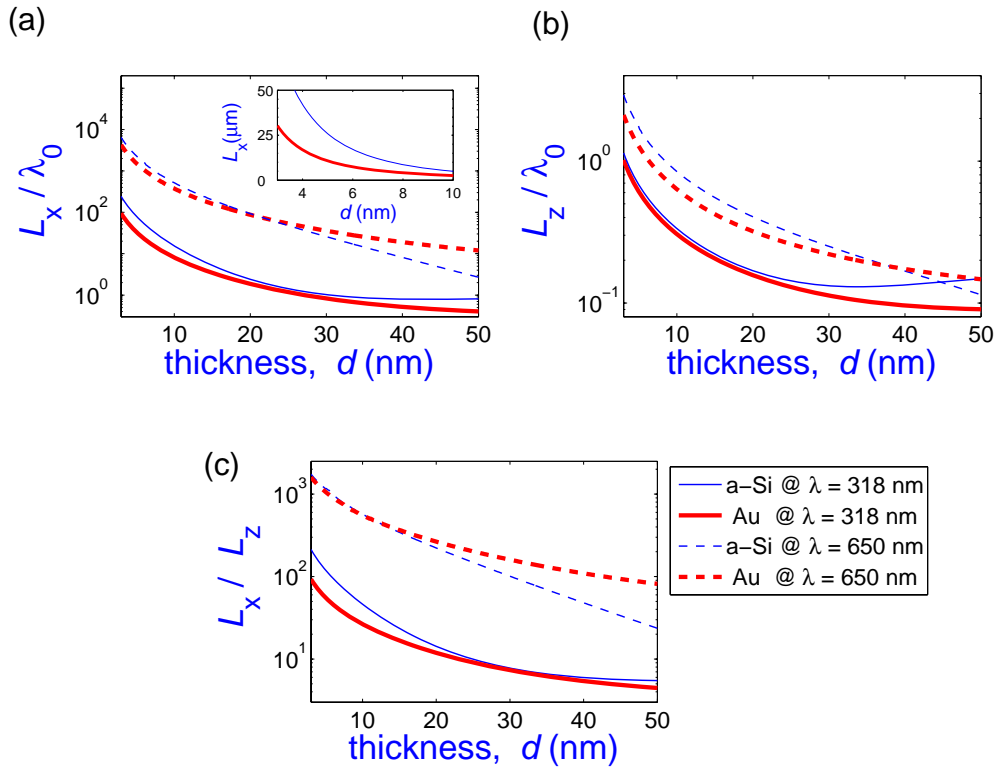


Fig. 3. (a) LRSP propagation length L_x normalized by λ_0 in a film of thickness d of gold (thick red curves) and silicon (thin blue curves) surrounded by a dielectric with refractive index $n_d = 1.45$. The solid curves correspond to $\lambda_0 = 318$ nm, while the dashed curves are the calculations for $\lambda_0 = 650$ nm. The inset represents a close view of L_x at $\lambda_0 = 318$ nm for small values of d . (b) decay length of the field intensity L_z (normalized by λ_0) in the dielectric for the same materials and wavelength as in (a). (c) Figure of merit of thin-film guiding structures defined as L_x/L_z for the same materials and wavelengths as in (a).

electromagnetic field in the case of an a-Si thin film in a SiO_2 medium at $\lambda_0 = 318$ nm. This calculation is presented in Fig. 4. Note that, for clarity, different scales have been used for the different layers. The poynting vector is strongly reduced inside the absorbing layer and it extends into the non-absorbing SiO_2 surrounding medium. Therefore, the electromagnetic energy density is mainly confined in the loss-less material and the surface polariton can propagate with reduced losses.

3. Long-range surface polaritons on thin a-Si films

We have investigated experimentally the excitation of LRSPs at UV and visible frequencies in thin films of a-Si. Two samples were prepared, the first one is an a-Si film with a thickness of 13 nm sputtered onto a SiO_2 substrate and covered by 350 nm of SiO_2 . The second sample consists of an a-Si film with thickness of 20 nm covered by 500 nm of SiO_2 . A scanning electron microscope side view image of the first sample is shown in Fig. 5.

The excitation of LRSPs in the films of a-Si was investigated with attenuated total reflection measurements. Due to momentum mismatch, it is not possible to couple free space light

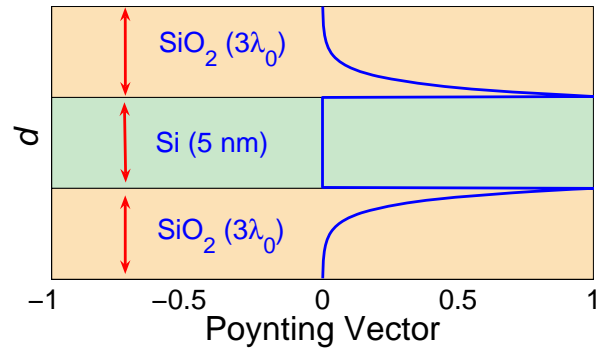


Fig. 4. LRSP's Poynting vector component tangential to an a-Si thin-film. The thickness of the a-Si is $d = 5$ nm with permittivity $\epsilon = 18.5i$ at $\lambda_0 = 318$ nm, and the background is SiO_2 . Note that, for clarity, the scales for the SiO_2 layer and the a-Si film are different.

to LRSPs in a thin film below a critical thickness. A prism with a higher permittivity than the dielectric surrounding the thin film can be used to match the momentum of the incident light to the momentum of LRSPs. In our experiments we used a prism of F2 Schott optical glass placed on top of the samples. The specular reflection at the prism- SiO_2 interface was measured for different angles of incidence and at different wavelengths. The incident beam is totally internally reflected at angles larger than the critical angle of the prism- SiO_2 interface. However, the evanescent transmitted field can resonantly couple to LRSPs at certain angles and wavelengths. This coupling to LRSPs leads to the reduction of the reflected intensity.

The experiments were done in a computer controlled rotation stage set-up that allowed the simultaneous rotation of sample and detector. We used a pulsed diode laser (Picoquant PDL 800-B) emitting at a wavelength $\lambda_0 = 375$ nm and a Si photodiode as detector to investigate the UV excitation of LSRPs. We also used a collimated beam from a halogen lamp (Yokogawa AQ4303) and a fiber coupled spectrometer (Ocean Optics USB2000) to perform broadband measurements at optical frequencies. The angle of incidence was varied by rotating the sample in steps of 0.05 degrees.

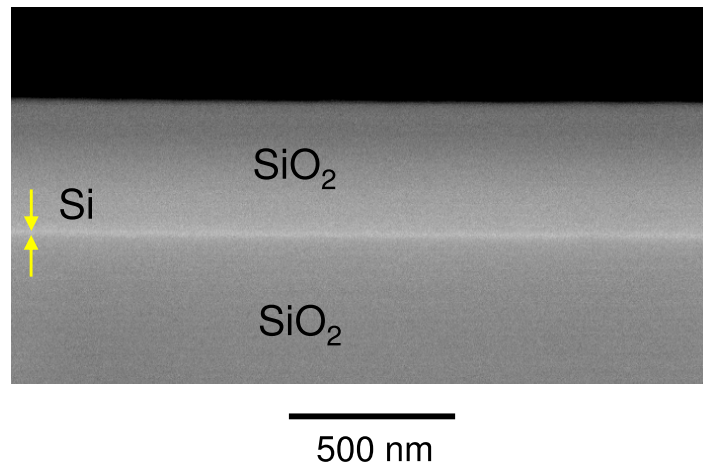


Fig. 5. (a) Side view image, made with a scanning electron microscope, of an a-Si thin film sputtered onto a SiO_2 substrate and covered by a SiO_2 layer.

Figure 6(a) displays a reflectivity measurement of a p -polarized beam of the halogen lamp on the sample formed by the a-Si film of 20 nm. Calculations of the reflectivity are presented in Fig. 6(b). The increase of reflectivity close to $\theta = 62^\circ$ at long wavelengths corresponds to the total internal reflection at the critical angle on the prism-SiO₂ interface. The excitation of guided modes in the a-Si is manifested by the narrow band of low reflectivity around 63.5° and $\lambda_0 \simeq 550$ nm. This band actually covers the transition between a LRSPs due to high absorption in a-Si at short wavelengths ($\epsilon \approx 17 + 15i$ at $\lambda_0 = 450$ nm) to the TM₀ mode in a weakly absorbing a-Si layer at long wavelengths ($\epsilon \approx 16 + 2.4i$ at $\lambda_0 = 700$ nm). As previously pointed by Yang *et al.* in Ref. [19] and as can be appreciated in Fig. 6, there is not a drastic transition between LRSPs and the TM₀ mode as the absorption in the thin film increases.

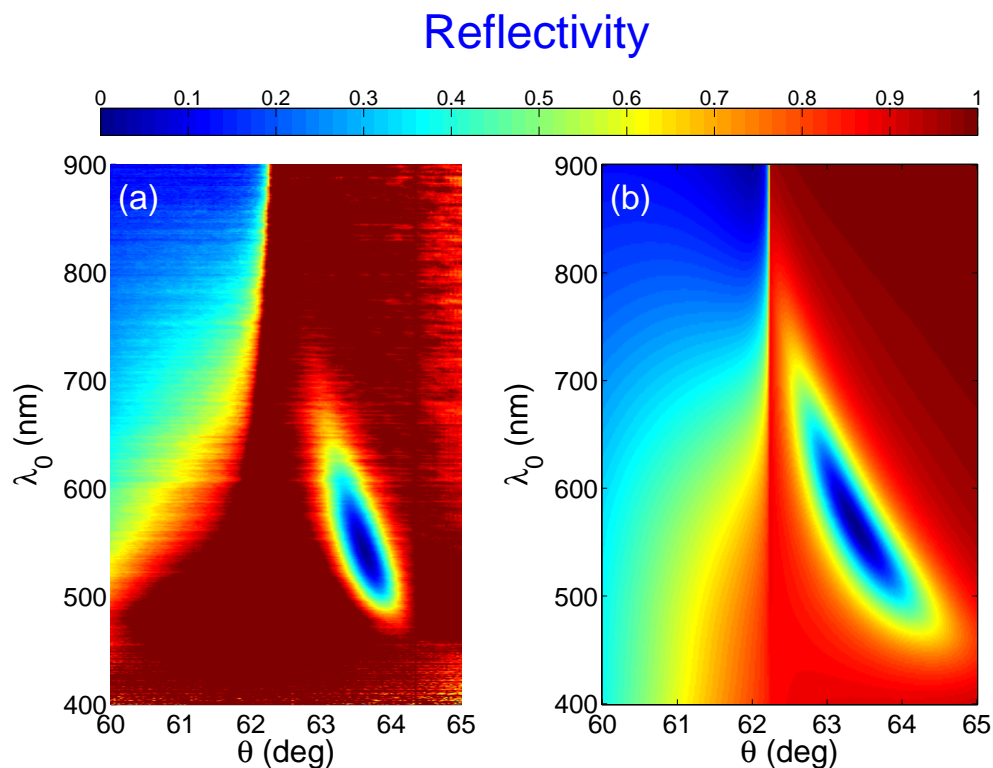


Fig. 6. (a) Measurements and (b) calculations of the reflected spectra of p -polarized light incident at an angle θ on the system formed by F2 glass, a SiO₂ layer with a thickness of 500 nm, a 20 nm layer of a-Si and a SiO₂ substrate.

The resonant frequency of excitation to LRSPs can be tuned by varying the coupling between surface polaritons at the opposite interfaces of the absorbing film. This tuning can be achieved by changing the thickness of the film and the SiO₂ layer on top. Figure 7 displays measurements at $\lambda_0 = 375$ nm (circles) and calculations (curves) of the reflection of the a-Si layer with a thickness of 13 nm covered by a SiO₂ layer of 350 nm. The theoretical curves were obtained by leaving the thickness of the SiO₂ and a-Si layers as free parameters to fit to the measurements. The permittivities of a-Si and SiO₂ were determined by ellipsometry measurements (not shown here) on a-Si layer with the same thickness and on a SiO₂ substrate, and were kept fixed in the fits. Within the experimental accuracy, the values of the permittivity of the thin film of a-Si were in agreement with those of bulk a-Si [30], and electronic quantum confinement perpendicular

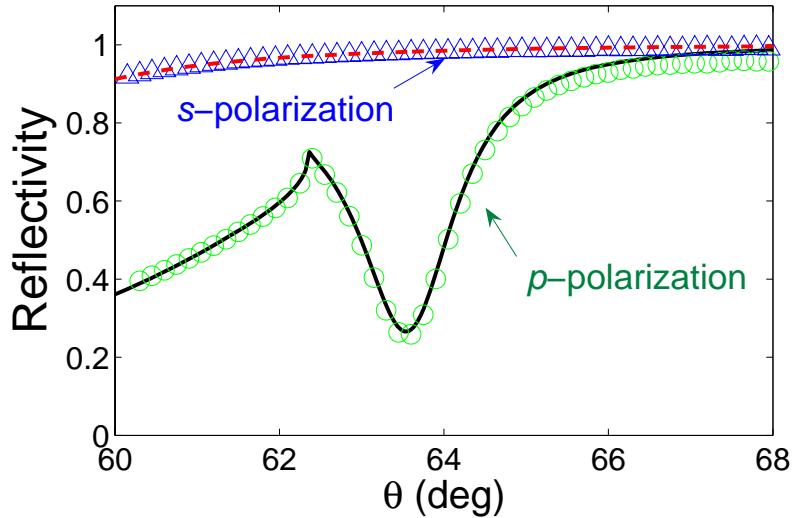


Fig. 7. Experimental (open circles and triangles) and theoretical (curves) reflectivity at $\lambda_0 = 375$ nm of the system formed by F2 glass, a SiO_2 layer with a thickness of 345 nm, an a-Si layer with a thickness of 13 nm and a SiO_2 substrate. The green circles and solid black curve correspond to p -polarized light, while the blue triangles and red dashed curve correspond to s -polarized light.

to the layer plane could be neglected. The values of the thickness of the SiO_2 layer, 13 nm, and of the a-Si layer, 345 nm, obtained from the fits are in agreement with the SEM image of Fig. 5.

The measurement and calculation of the p -polarized reflection (green circles and black curve in Fig. 7) have a sharp dip at an angle $\theta = 63.6^\circ$, larger than the critical angle of total internal reflection ($\theta_c \simeq 62^\circ$). At $\theta = 63.6^\circ$ the momentum of the evanescent transmitted beam through prism- SiO_2 interface matches the momentum of the LRSP and coupling is possible, giving rise to the reduction of the reflection. For $\lambda_0 = 375$ nm the absorption in a-Si is very strong ($\epsilon = 10.8 + 19.9i$) and this minimum in the reflection can be attributed to coupling to LRSPs. No particular features are found in the s -polarization (blue triangles and red dashed curve in Fig. 7), as for this polarization and configuration it is not possible to excite LRSPs.

An important aspect which determines the propagation length of long range guided modes in thin films is the surface roughness. We have determined this roughness by performing atomic force microscopy measurements (not shown) on a similar layer of sputtered a-Si with a thickness of 12.5 nm on top of a SiO_2 substrate. These measurements lead to a root mean square value of the surface roughness of only 0.35 nm, which was mainly determined by the substrate. The effect of the roughness in thin films of a-Si on the propagation length of LRSPs is therefore negligible. Note that, due to the formation of islands, reported values of the surface roughness of similar thin films of gold are one order of magnitude larger [33]. Consequently, ultra-thin layers of a-Si have better characteristics than gold layers for the propagation of long-range surface polaritons.

As mentioned above, the position and depth of the resonance shown in Fig. 7 are very sensitive to variations in thickness of the a-Si and SiO_2 layers. If we consider a system assuming a 10 nm a-Si film and a 300 nm SiO_2 top layer, it is possible to obtain perfect coupling to LRSPs as is shown in the calculation displayed in Fig. 8. The blue solid curves in Fig. 8(a) and 8(b) represent calculations of the attenuated total reflection of p -polarized light ($\lambda_0 = 375$ nm) incident onto this system of optimized dimensions. For this structure the reflection vanishes

at $\theta = 62.9^\circ$ indicating a 100% coupling efficiency to LRSPs. Figure 8(c) displays a calculation of the magnetic field amplitude, i.e., the only field component in the y-direction, for a p -polarized incident beam at 62.9° . Only the incident field is present in the prism (upper part of the plot), as can be appreciated by the absence of interference that would point to specular reflection in the prism-SiO₂ interface. This vanishing reflection arises from the perfect coupling of the evanescent field transmitted into the SiO₂ layer to LRSPs in the thin a-Si layer. The maximum field amplitude of the LRSP in Fig. 8(c) is at the surface of the a-Si film and decays evanescently from this layer into the surrounding dielectric. For clarity, we display on Fig. 8(d) with a red solid curve a vertical cut at $x = 0$ of the contour plot 8(c). To make the a-Si layer visible, we have scaled its thickness in this figure. The oscillatory amplitude on the upper part of the figure corresponds to the incident field in the prism. We can see a small dip in the magnetic field amplitude in the center of the a-Si thin film and the exponential amplitude decay in the surrounding SiO₂ characteristic of a surface wave. The electric field amplitude component along the x direction at $x = 0$ is also represented in Fig. 8(d) with a black dashed line. This field amplitude is asymmetric with respect to the middle plane of the thin film, as it is expected for long range surface polaritons [19].

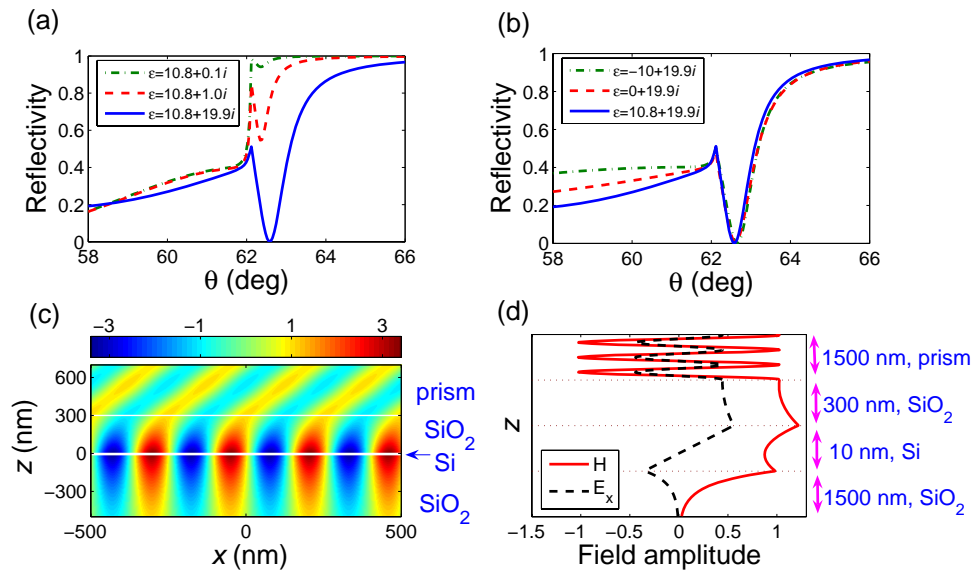


Fig. 8. (a) and (b) display the reflectivity at $\lambda_0 = 375$ nm of a sample formed by a prism ($n_{\text{prism}} = 1.67$) on top of a SiO₂ layer with a thickness of 300 nm, an a-Si layer with a thickness of 10 nm and a SiO₂ substrate ($n = 1.48$). The reflectivity is calculated for different values of the imaginary part (a) and the real part (b) of the permittivity of the thin layer. The full blue curves in (a) and (b) are calculated for $\epsilon = 10.8 + 19.9i$, i.e., the dielectric constant of a-Si at $\lambda_0 = 375$ nm. In figure (a) $\epsilon = 10.8 + 1.0i$ (red dashed curve) and $\epsilon = 10.8 + 0.1i$ (green dot-dashed curve). In figure (b) $\epsilon = 0 + 19.9i$ (red dashed curve) and $\epsilon = -10 + 19.9i$ (green dot-dashed curve). (c) Calculation of the magnetic field amplitude for a p -polarized beam ($\lambda_0 = 375$ nm) incident at 62.9° onto the sample with the same dimensions as in (a) and (b). Magnetic field amplitude (red full curve) and x -component of the electric field (black dashed curve) at $x = 0$ are shown in (d). Note that, for clarity, the SiO₂ layer and the silicon film are scaled.

In order to highlight the relevance of the imaginary permittivity of the thin film for the excitation of LRSPs, we have calculated the attenuated total reflection for different values of ϵ_i ; keep-

ing ϵ_r constant. These results correspond to $\epsilon = 10.8 + 1.0i$ for the red dashed curve in Fig. 8(a) and $\epsilon = 10.8 + 0.1i$ for the green dot-dashed curve. The LRSP resonance vanishes as the absorption in the thin film is reduced. If, on the other hand, the real component of the permittivity is varied the LRSPs remains unchanged. This is illustrated in Fig. 8(b) where the attenuated total reflection of the thin layer of absorbing material is calculated for values of the permittivity of $\epsilon = 10.8 + 19.9i$ (blue curve), $\epsilon = 0 + 19.9i$ (red dashed curve) and $\epsilon = -10 + 19.9i$ (green dot-dashed curve). The results of Fig. 8(a) and Fig. 8(b) can be summarized by saying that LRSPs are excited in thin films of strongly absorbing layers embedded in non-absorbing dielectrics independently of the value of the real part of the permittivity of the absorbing layer. This is in contrast to TM_0 modes and long-range surface plasmon polaritons, which mainly depend on this value of the real part of the permittivity.

4. Conclusions

We have demonstrated the excitation of long-range surface polaritons LRSPs in ultra-thin films of amorphous silicon at visible and UV frequencies. These modes have similar characteristics to long-range surface plasmon polaritons and TM_0 modes with the important difference that LRSPs are sustained by thin layers of strongly absorbing media while surface plasmon polaritons and TM_0 are supported by thin layers of metals and non-absorbing dielectrics respectively. Excitation of long-range surface modes in absorbing Si opens the possibility to surface polariton optics compatible with standard Si processing technology.

Acknowledgments

We acknowledge J. H. J. Roosen, M. M. M. Vervest and A. P. M. de Win for technical assistance, and J.A. Sánchez-Gil and M. Verschuuren for stimulating discussions. This work was supported by the Netherlands Foundation Fundamenteel Onderzoek der Materie (FOM) and the Nederlandse Organisatie voor Wetenschappelijk Onderzoek (NWO), and is part of an industrial partnership program between Philips and FOM.